Chapter 4 Microwave Sensors

4.1 Types of Microwave Sensor

There are two types of microwave sensors, passive and active. Table 4.1.1 shows the typical microwave sensors and targets to be measured.

Table 4.1.2 shows the frequency of passive microwave sensor for monitoring major targets. Table 4.1.3 shows the frequency of active microwave sensor for monitoring major targets.

Many of the earth observation satellites to be launched after 1992 are planned to have microwave sensors onboard. Active sensors will be classified into more types in terms of the target with respect to horizontal or vertical polarization.

Table 4.1.1 Microwave remote sensor

Sensor		Target
Passive sensor	Microwave Radiometer	near sea surface wind sea surface temperature state of sea salinity, sea ice water vapor, cloud water content precipitation intensity air temperature, wind ozone, aerosol, NOx other atmospheric components
Active sensor	Microwave Scatterometer	soil moisture content surface roughness distribution of lake ice distribution of sea ice distribution of snow biomass sea surface temperature state of sea water vapor precipitation intensity ocean wave near sea surface wind wind direction and velocity
	Microwave Altimeter	sea surface topography, geoid ocean wave-height change of ocean current meso-scale eddy, tide wind velocity
	Imaging Radar	image of surface ocean wave near sea surface wind, wind topography and geology submarine topography monitoring of ice

Table4.1.2 Frequency of active microwave sensor for monitoring major target.[1)]

frequency(GHz)	monitoring target
around 1.4	soil moisture content, salinity
around 2.7	salinity, soil moisture content
around 5	temperature of estuary
around 6	sea surface temperature
around 11	rain, snow, lake ice, sea surface condition
around 15	water vapor, rain
around 18	rain, sea surface condition, sea ice, water vapor
around 21	water vapor, liquid water
22.24	water vapor, liquid water
around 24	water vapor, liquid water
around 30	sea ice, water vapor, oil slick, cloud, liquid water
around 37	rain, cloud, sea ice, water vapor
around 55	temperature
around 90	cloud, oil slick, ice, snow
100.49	NOx
110.80	ozone
115.27	CO
118.70	temperature
125.61	NOx
150.74	NOx
164.38	ClOx
167.20	ClOx
175.86	NOx
183.31	water vapor
184.75	ozone
200.98	NOx
226.09	NOx
230.54	CO
235.71	ozone
237.15	ozone
251.21	NOx
276.33	NOx
301.44	NOx
325.10	water vapor
345.80	CO
364.32	ozone
380.20	water vapor

Table 4.1.3 Frequency of active microwave sensor for monitoring major target.[1)]

frequency(GHz)	monitoring target
around 1	ocean waves
around 3	geology
around 5	soil moisture content
around 10	rainfall
around 14	wind,ice,geoid
around 17	vegetation
around 35	snow
around 75	cloud

4.2 Real Aperture Radar

Imaging radar as shown in Table 4.1.1 is classified further into **real aperture radar** (RAR) and synthetic aperture radar (SAR). In this section RAR is explained.

RAR transmits a narrow angle beam of pulse radio wave in the **range direction** at right angles to the flight direction (called the **azimuth direction**) and receives the backscattering from the targets which will be transformed to a radar image from the received signals, as shown in Figure 4.2.1.

Usually the reflected pulse will be arranged in the order of return time from the targets, which corresponds to the range direction scanning.

The resolution in the range direction depends on the pulse width, as shown in Figure 4.2.2. However if the pulse width is made small, in order to increase the resolution, the S/N ratio of the return pulse will decrease because the transmitted power also becomes low. Therefore, the transmitted pulse is modulated to chirp with a high power but wide band, which is received through a **matched filter,** with reverse function of transmission, to make the **pulse width** very narrow and high power as shown in Figure 4.2.3. This is called **pulse compression** or **de-chirping**. By making the pulse compression, with an increase of frequency f in transmission, the amplitude becomes $\sqrt{T.\Delta f}$ times bigger, and the pulse width becomes $1/T\Delta f$ narrower. This method is sometime called range compression.

The resolution in the azimuth direction is identical to the multiplication of beam width and the distance to a target. As the resolution of azimuth direction increases with shorter wave length and bigger antenna size, a shorter wavelength and a bigger antenna is used for higher azimuth resolution, as shown in Figure 4.2.4.

However as it is difficult to attach such a large antenna, requiring for example a 1 km diameter antenna in order to obtain 25 meters resolution with L band (λ=25 cm) and 100 km distance from a target, a real aperture radar therefore has a technical limitation for improving the azimuth resolution.

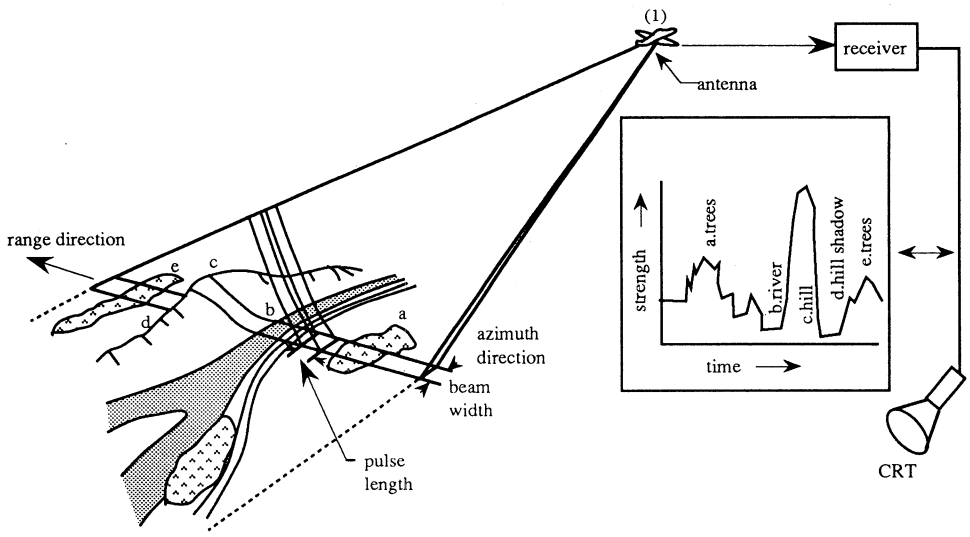

Figure 4.2.1 Side-looking airborne radar operation

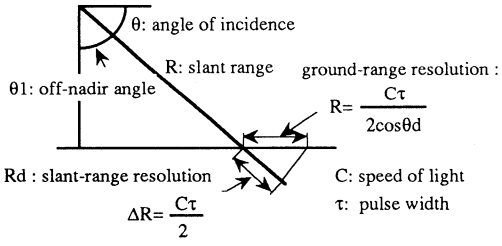

Figure 4.2.2 Range resolution

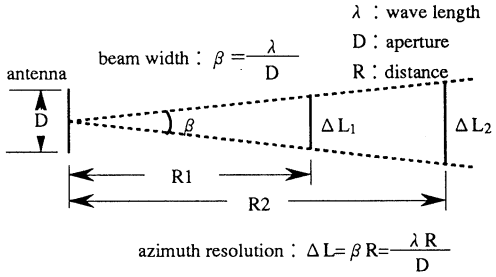

Figure 4.2.4 Illustration of azimuth resolution

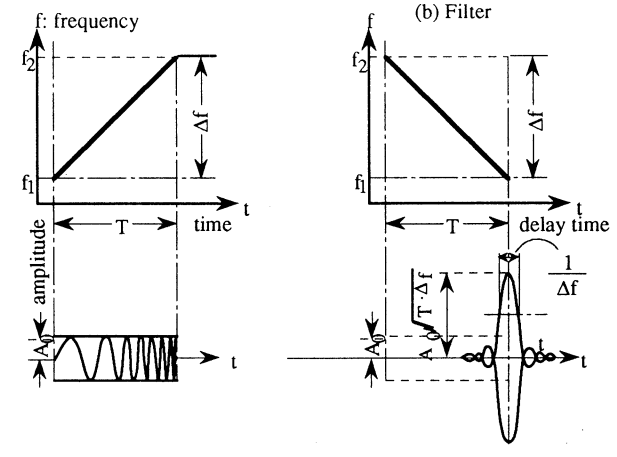

Figure 4.2.3 Principle of pulse compression

4.3 Synthetic Aperture Radar

Compared to real aperture radar, **synthetic aperture radar** (SAR) synthetically increases the antenna's size or aperture to increase the azimuth resolution though the same pulse compression technique as adopted for range direction. Synthetic aperture processing is a complicated data processing of received signals and phases from moving targets with a small antenna, the effect of which is to should be theoretically convert to the effect of a large antenna, that is a **synthetic aperture length**, as shown as Figure 4.3.1.

The synthetic aperture length is the beam width by range which a real aperture radar of the same length, can project in the azimuth direction.

The resolution in the azimuth direction is given by half of real aperture radar as shown as follows.

Real beam width : $\beta=\lambda /D$

Real resolution: $\Delta L=\beta \ R=Ls$ (synthetic aperture length)

Synthetic beam width : $\beta s = \lambda / 2Ls= D / 2R$

Synthetic resolution : $\Delta Ls = \beta sR = D / 2$

where λ :wavelength D: aperture of radar R: slant range

This is the reason why SAR has a high azimuth resolution with a small size of antenna regardless of the slant range, or very high altitude of a satellite.

Figure 4.3.2 shows the basic theory of SAR or synthetic aperture processing including the Doppler effect, matched filter and azimuth compression.

SAR continues to receive return pulses from a target during the time the radar projects the beam to the target. In the meanwhile the relative distance between the radar and the target changes with the movement of the platform, which produces a Doppler effect to modulate a chirp modulation of received pulse. A matched filter corresponding to the reverse characteristics of chirp modulation will increase the azimuth resolution of azimuth direction. This is called **azimuth compression**.

In the case of SAR, unsuitability of satellite velocity and attitude will reduce the effect of the Doppler effect. Therefore the satellite with SAR is required to be high, because the correction for synthetic aperture processing due to instability at lower altitudes is very difficult.

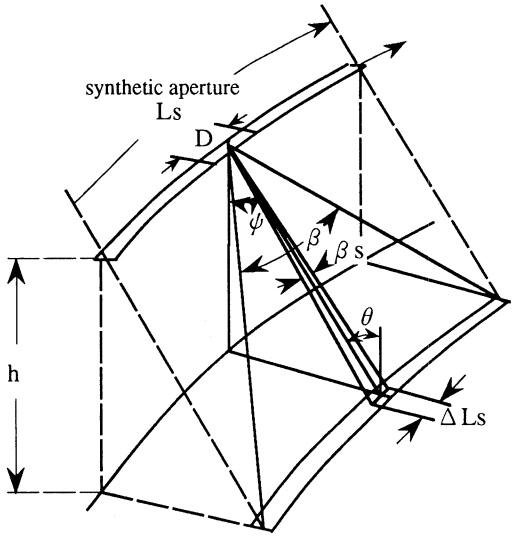

D : real aperture
β : real beam width
β s : synthetic beam width
h : height
Δ Ls : azimuth resolution
ψ : off nadir angle

Figure 4.3.1 Relation between real aperture and synthetic aperture radar

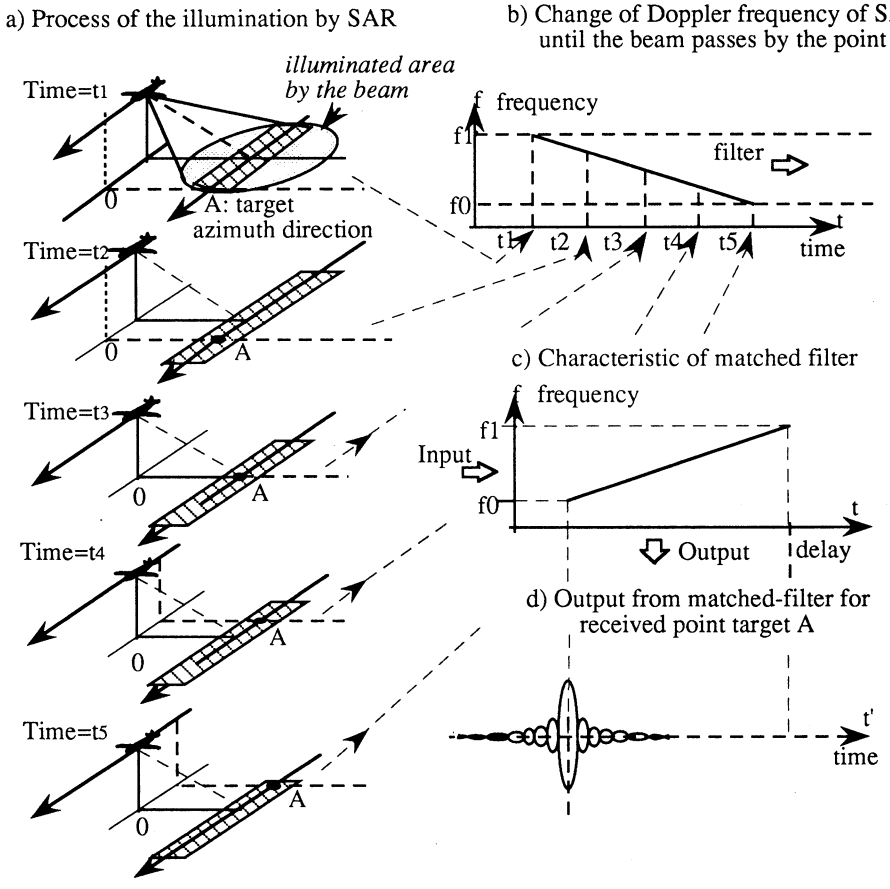

Figure 4.3.2 Basic theory of SAR using Doppler beam-sharpening(modified Fig.9.2 in 1)

4.4 Geometry of Radar Imagery

The incident angle of microwave to a target is the angle from the normal line while the **aspect angle** is the supplementary angle as shown in Figure 4.4.1. The smaller the incident angle , the larger the back scattering intensity .

Off nadir angle is the angle between the microwave and the nadir, while the depression angle is the angle from the horizon, as shown in Figure 4.4.2. There occurs a geometric distortion or shadow depending on the relationship between the off nadir angle and the terrain relief, as shown in Figure 4.4.3 and Figure 4.4.4. **Foreshortening** occurs when the **ground range** difference (horizontal distance ΔX) is reduced to the **slant range** difference ΔR, because the slant range to the top and the bottom are not proportional to the horizontal distances, as shown in the right hand example of Figure 4.3.3.

When the shortening becomes greater, the image of the top of a feature such as a mountain will be closer to the antenna than the bottom, which causes loss of, the slope image, as shown in the left hand example of Figure 4.3.3. This is called **layover**.

Such phenomena will occur when the terrain relief is greater and the off nadir angle is smaller.

However for large off nadir angles, there will be a shadow area, as called radar shadow, behind a hill or mountain, which makes the image very dark as shown in Figure 4.3.4.

The **radar shadow** will occur if the following relationship is satisfied.

$$\alpha + \theta > 90$$

where α: slope angle of back slope

θ: off nadir angle

The slant range of the shadow is given as sec θ as shown in Figure 4.4.4.

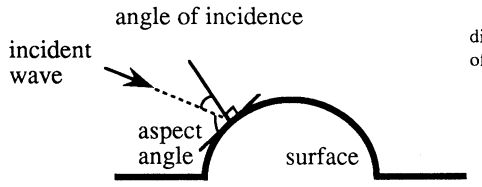

Figure 4.4.1 Angle of incidence and aspect angle

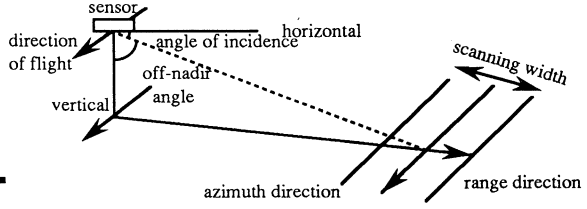

Figure 4.4.2 Off-nadir angle

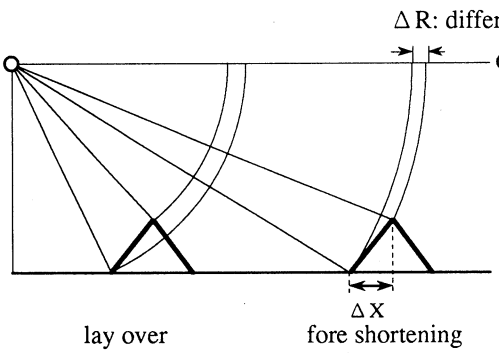

Figure 4.4.3 Fore shortening and lay over

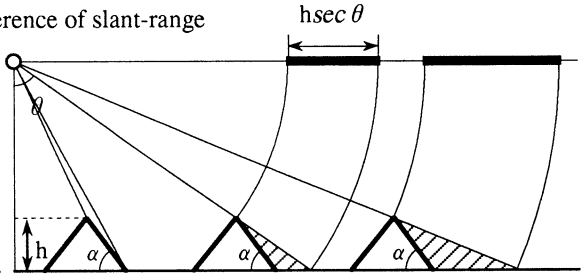

Figure 4.4.4 Radar shadow

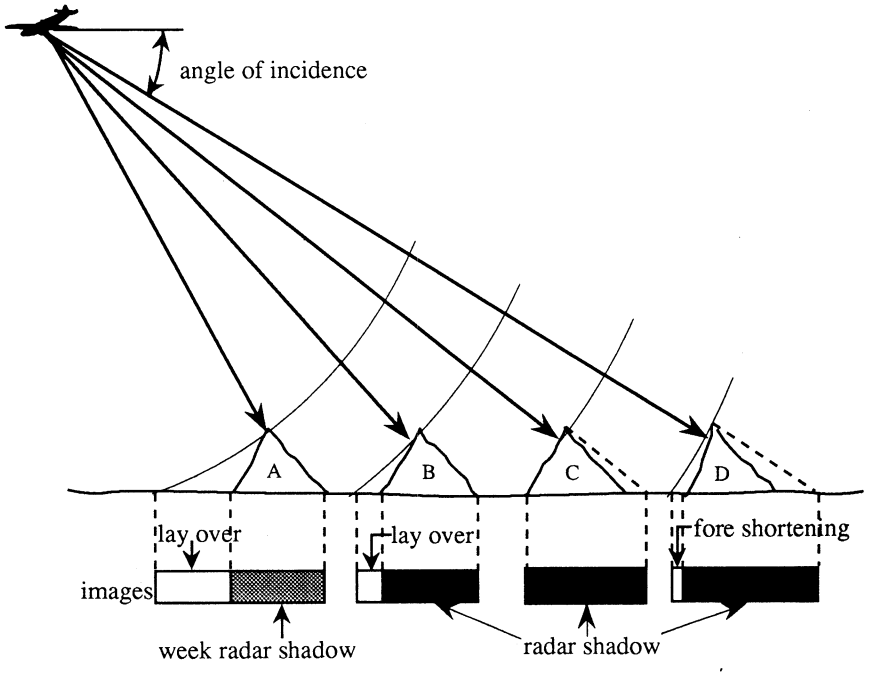

Figure 4.4.5 Geometric distortions in SAR images

4.5 Image Reconstruction of SAR

Raw data from SAR are records of backscattering in time sequence which are returned from the ground targets. Return signal from a point P is recorded in the expanded range in the range direction which is identical to the pulse width. In addition, the return signal from a point P is also expanded in the azimuth direction because the point P continues to be radiated by microwave pulses during the flight motion.

Data processing to generate an image of gray tone corresponding to the backscattering intensity of each point on the ground is called image reconstruction of synthetic aperture radar (SAR). Figure 4.5.3 shows the flow of image construction of SAR.

The image reconstruction is divided into range compression and azimuth compression which make compression of expanded signals in both range and azimuth directions into a point signal. The compression is usually carried out by adopting Fourier transformation to achieve convolution of received signals and a **reference function**.

The reference function of range compression is the complex conjugate of the transmitted signal, while the reference of azimuth compression is a complex conjugate of the modulated signal by chirp modulation.

The slant range to a point on the ground is expressed as the quadratic function of time with respect to the movement of the platform. The change of the slant range is called **range migration**. The first order term is called **range walk** resulting from the earth rotation, while the second order term is called **range curvature**.

The range migration correction is to relocate the quadratic distribution (see Figure 4.5.4 (c)), in which range walk and range curvature may be separately processed.

In image reconstruction, there is a major problem, called speckle which is due to high frequency noise, as seen in the example of Figure 4.5.2. In order to reduce the speckle, **mulch-look processing** is applied in which range compression and azimuth compression with respect to subdivided frequency domains are independently overlaid three or four times termed the number of looks. Sometimes a median filter or local averaging may be applied to reduce the speckle. The speckle will be reduced by the square root of the number of looks, although the spatial resolution declines in proportion to the number of looks.

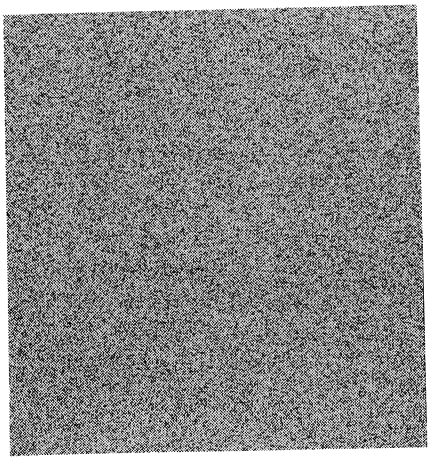

Figure 4.5.1 Example of row data of SAR

Figure 4.5.2 Example of reconstructed data of SAR

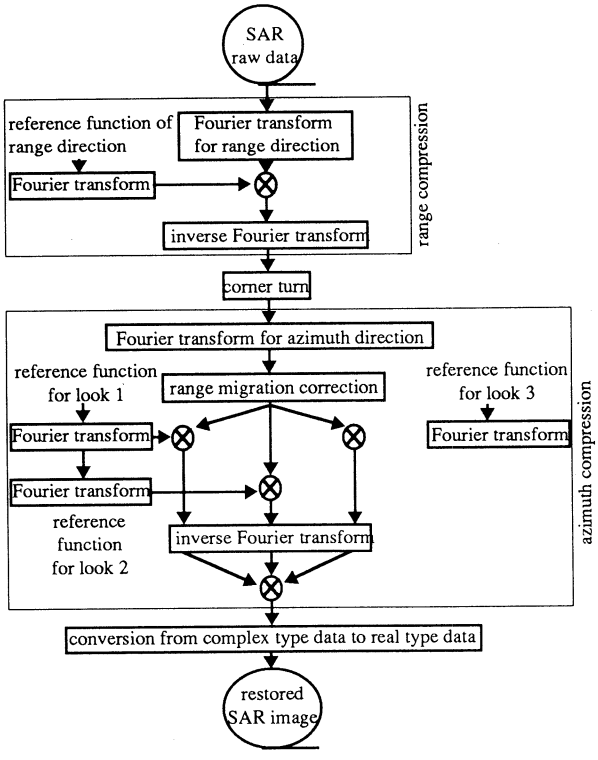

Figure 4.5.3 Reconstruction flow of SAR images (case of 3 looks)

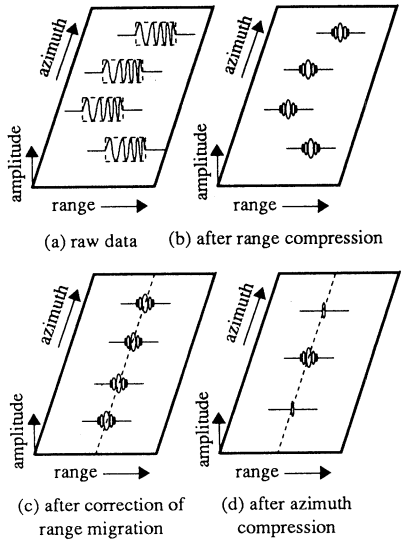

Figure 4.5.4 Concept of SAR image reconstruction (from view point of return signal from a point target)

4.6 Characteristics of Radar Image

The main objective of microwave remote sensing is to estimate the property of objects by interpreting the features of the radar image. Typical objects to be measured by microwave remote sensing are mountainous land forms, subsurface geology, sea wind and waves etc. In order to estimate these properties, it is very important to understand the effects of microwave backscattering on the objects.

Two factors of microwave characteristics are of importance; frequency (or wavelength) and polarization. In microwave remote sensing, various wavelengths (or frequency) such as L band, C band, X band, P band etc. will be used ranging from millimeter wavelengths (1 mm - 1cm) up to about 30 cm. According to the wavelength or frequency, specular reflection will occur, so that the surface roughness can be detected if multi-frequency radar images are compared.

Figure 4.6.1 - 4.6.3 are radar images of P band, L band and C band respectively with HH polarization, in which the difference of wavelength or frequency will provide different images.

Polarization is defined as the oscillating direction involved in an electric field. Usually transmitted microwave and received microwave will have a choice between horizontal polarization and vertical polarization. Therefore four combinations; HH, HV, VH and VV can be used for SAR. The backscattering characteristics are also different with respect to polarization. Figure 4.6.2, 4.6.4 and 4.6.5 are HH, HV, and VV combinations respectively with L band in which one can see different features.

In future, SAR systems with functions of multi-frequency and multi- polarization will be onboard earth observation satellites.

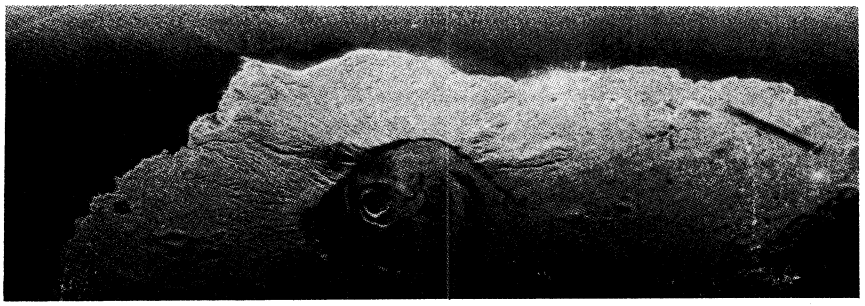

Figure 4.6.1 Image of Island Ooshima(Japan) by SAR-580(L-band(HH)) (height:6.1km Depression:40°)[1] (courtesy of NASDA)

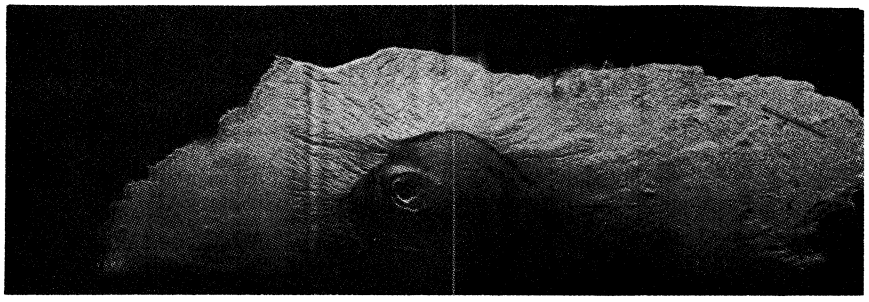

Figure 4.6.2 Image of Island Ooshima by SAR-580(X-band(HH)) (height:6.1km Depression:40°)[1] (courtesy of NASDA)

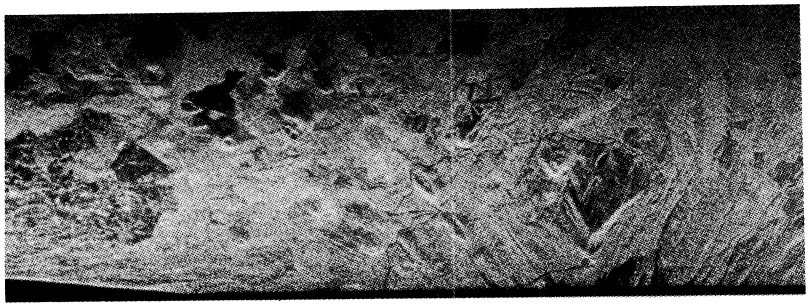

Figure 4.6.3 Image of the area around Mt.Fuji(Japan) by SAR-580(L-band(HH)) (height:6.1km Depression:40°)[1] (courtesy of NASDA)

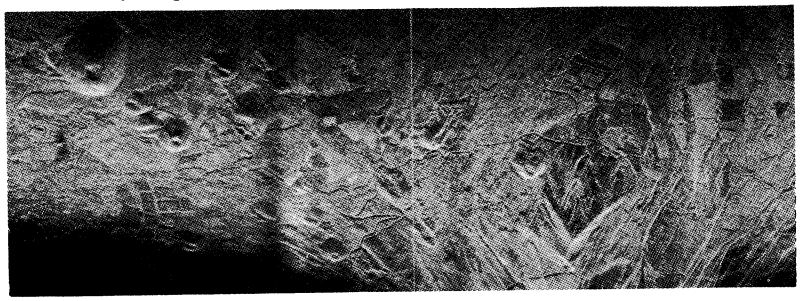

Figure 4.6.4 Image of the area around Mt.Fuji by SAR-580(X-band(HH)) (height:6.1km Depression:40°)[1] (courtesy of NASDA)

4.7 Radar Images of Terrains

The biggest effect of microwave backscattering on variations in the radar image is due to terrain features. It is larger than the effect of permittivity. Particularly the effect of incident beam angle in terms of off nadir angle and terrain slope will produce various effects such as foreshortening, layover and shadow as already explained in section 4.4.

Normally in the closer range from SAR, called **near range,** layover may occur while in the **far range** more shadow may be seen. This means that care should be taken with the flight direction and range direction in interpretation of terrain features.

Figure 4.7.1 shows an example of a SAR image of SEASAT around the mountainous areas of Geneva, Switzerland.

Figure 4.7.2 shows the effect of terrain and off nadir angle on foreshortening, layover and shadow.

Usually foreshortening and layover appear as a bright response around the summit or ridge, while shadow appears black without any information in the shadow area.

As seen in the figure, the effect of microwave back scattering can be better seen along the track or azimuth direction than in the cross track direction.

By interpreting the radar image, land form classification, lineament analysis, mineral resources exploration, monitoring of active volcanoes, land slide monitoring, geological structure analysis and so on can be carried out.

Two parallel flights may produce a stereo pair which will offer the elevation information on terrain features. Recent work is Canada has demonstrated that terrain elevation information can also be derived from the use of interferometry with a single flight line.

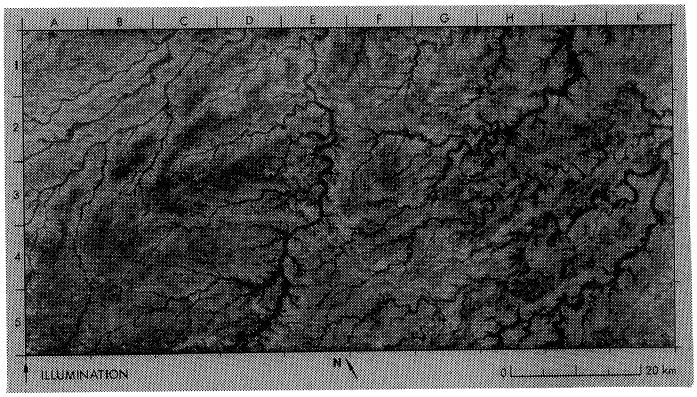

Figure 4.7.1 (a) Widyan, Saudi Arabia and Iraq / SIR-A img.1) (courtesy of NASA/JPL)

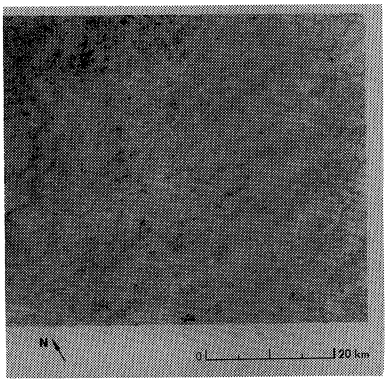

Figure 4.7.2 (b) Widyan, Saudi Arabia and Iraq / Landsat Band 7 img.1) (courtesy of NASA/JPL)

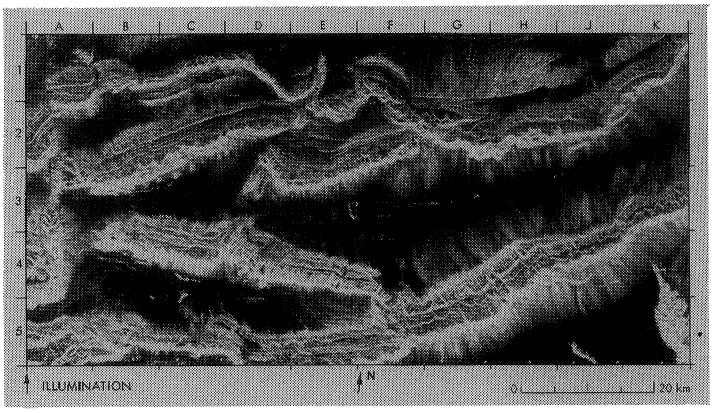

Figure 4.7.3 Kalpin Cholo and Chong Korm Mountains, Xinjiang, China / SIR-A img.1) (courtesy of NASA/JPL)

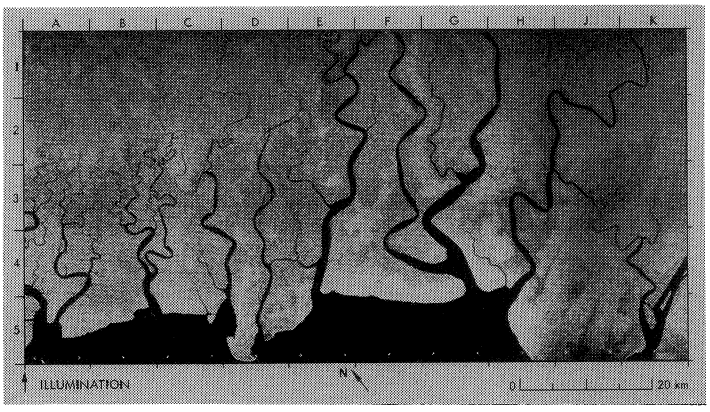

Figure 4.7.4 Southwest Coastal Swamp, Irian Jaya, Indonesia / SIR-A img.1) (courtesy of NASA/JPL)

4.8 Microwave Radiometer

As indicated in section 3.4, a part of the microwave is also radiated by thermal radiation from the objects on the earth. Microwave radiometers or passive type microwave sensors are used to measure the thermal radiation of the ground surface and/or atmospheric condition.

Brightness temperature measured by a microwave radiometer is expressed by Reyleigh-Jean's law (see 1.7), which is the resultant energy of thermal radiation from the ground surface and the atmospheric media. Multi-channel radiometers with multi- polarization are used to avoid the influences of unnecessary factors to measure the specific physical parameter.

Figure 4.8.1 shows the sensitivity of physical parameters in oceanography with respect to frequency and the optimum channels as arrow symbols.

Figure 4.8.2 shows two typical microwave scanning **radiometers**; the **conical scanning** type and the **cross track scanning** type. The former is used for the microwave channel which is influenced by the ground surface, while the latter is used for the channel which can be neglected by the influence of the ground surface.

The most simple radiometer is the total power radiometer, as shown in Figure 4.8.3 (a). This system has a mixer to enable it to mix high frequency of a local oscillator in order to amplify the high signal after transforming to a low frequency. However the influence of system gain variation cannot be neglected in this system.

The Dicke radiometer can reduce the influence of system gain variation by introducing a switch generator which allows it to receive the antenna signal and noise source of constant temperature, alternatively of which antenna signal can be detected later on, synchronously with the switch generator, as shown in Figure 4.8.3 (b).

The zero-balance Dicke radiometer can reduce the influence of system gain variation and increase the sensitivity further by adding a noise generator to the Dicke radiometer in order to increase the sensitivity about two times higher than total power radiometer, as shown in Figure 4.8.3 (c).

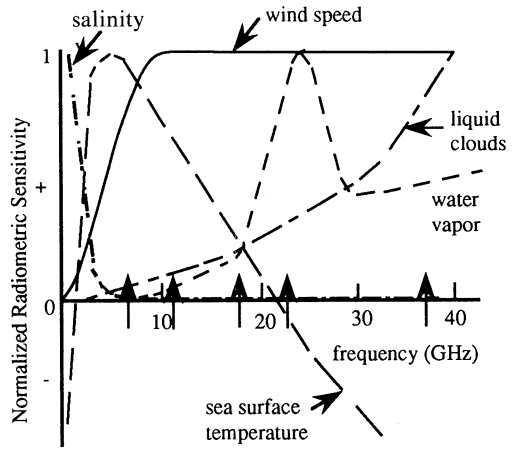

Figure 4.8.1 Sensitivity of physical parameters in oceanography with respect to frequency and the optimum channels as symbols arrow.[1)]

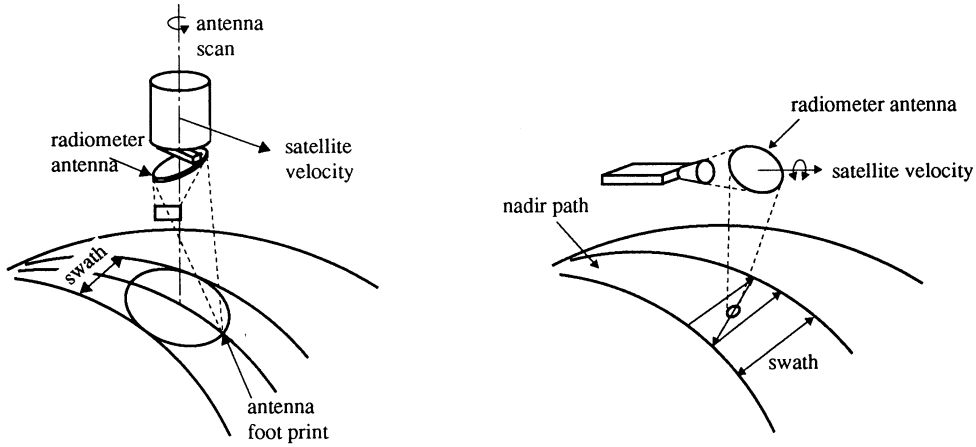

Figure 4.8.2 Microwave scanning radiometer[2)]

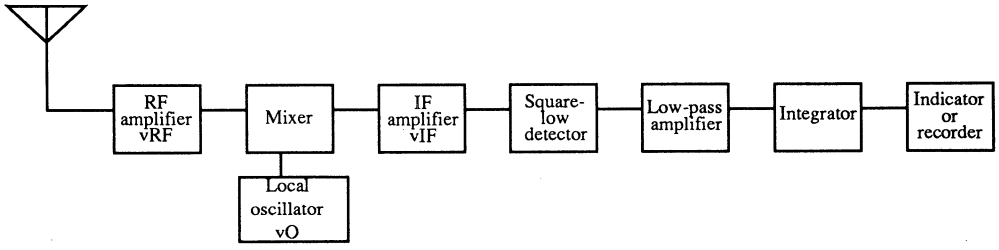

Figure 4.8.3 Total power radiometer system.[3)]

4.9 Microwave Scatterometer

Microwave scatterometers can measure the received power of surface backscattering reflected from the surface of objects. According to a narrow definition, a microwave scatterometer may be a space borne sensor to measure the two dimensional velocity vectors of the sea wind, while according to the wider definition, it also involves air-borne sensors, as well as ground based sensors to measure the surface backscattering as well as volume scattering, such as rain radar.

Microwave scatterometers are classified as two types, **pulse type** and **continuous wave type (CW)**. The pulse type uses wide band which has restrictions in obtaining a license to operate and in avoid obstructions. CW type has the advantage that the band width can be reduced to 1/100 times that of the pulse type and the price becomes cheaper.

SEASAT-SASS (Seasat-A Satellite Scatterometer) is one of the typical scatterometers. SASS has four fixed antennas to transmit the pulse in a fan beam of 14.5 GHz to four different angles, and to receive the backscattering in subdivided cells through a Doppler filter. Figure 4.9.1 shows the four beam patterns and the incident angles. In accordance with the satellite flight, the same cell of sea area can be observed from both fore beam and aft beam with 90° different angle, which enables the determination of wind direction and wind velocity.

Figure 4.9.2 shows a ground based microwave scatterometer with a rotation system.

ERS-1-AMI Wind Mode (European Remote Sensing Satellite-1-Active Microwave Instrument) and **ADEOS-NSCAT** (Advanced Earth Observation System-1 NASA Scatterometer) will be available for measurement of velocity vectors of the sea wind with three antennas looking fore, side and aft directions.

Table 4.9.1 compares the basic functions of ERS-AMI Wind Mode and ADEOS-NSCAT. Both have functions to measure wind velocity of the sea wind with an accuracy of 2 m/s or 10 % of the waveheight , and wind direction with an accuracy of 20°.

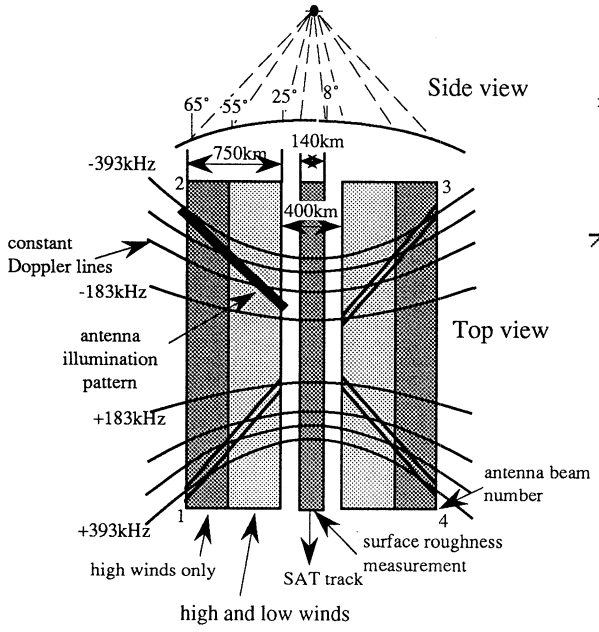

Figure 4.9.1 Seasat SASS fan-beam coverage

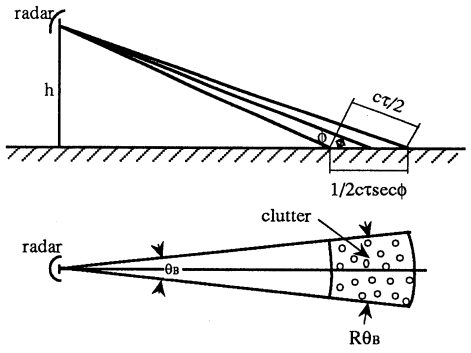

θB: beam width
c: speed of light (c=0.3million km/sec)
τ: pulse width
φ: incident angle
R: distance from radar to target

Figure 4.9.2 Principle of ground-based radar

Table 4.9.1 Basic function of ERS-AMI and ADEOS-NSCA

Scatterometer	(AMI(ERS-1)wind mode)	ADEOS(NSCAT)
Frequency	5.3GHz	14GHz
Polarization	VV	HH/VV
Spatial resolution	50km(25km Grid)	50km
Swath	400km	1200km
Beam direction	45°, 90° , 135°	±45°, ±135°, 65°, -115°
Wind speed range	4-24m/s	3-30m/s
Wind speed accuracy	2m/s or 10%	2m/s or 10%
Wind vector range	0-360°	0-360°
Wind vector directions accuracy	20°	20°

4.10 Microwave Altimeter

Microwave altimeters or radar altimeters are used to measure the distance between the platform (usually satellite or aircraft) and the ground surface. Some applications of microwave altimetry are in ocean dynamics of the sea current, geoid surveys, and sea ice surveys. Therefore, precise measurement of the satellite orbit and the **geoid** should be carried out.

The principle of satellite **altimetry** is shown in Figure 4.10.1. The ground height or the sea surface height is measured from the **reference ellipsoid**. If the altitude of the satellite Hs is given as the height from the reference ellipsoid, the **sea surface height** HSSH is calculated as follows.

$$H_{SSH} = Hs - Ha$$

where Ha : measured distance between satellite and the sea surface.

The sea surface height is also represented by the geoid height Hg that is measured between the geoid surface and the reference ellipsoid and the **sea surface topography** ΔH is given as follows.

$$H_{SSH} = Hg + \Delta H$$

The sea surface topography results from ocean dynamics such as sea current, wave height, tidal flow etc., which can be determined if the geoid height Hg is given. The distance between a satellite and the ground surface or sea surface; Ha, is measured on the basis of the travel time of the transmitted microwave pulses. From the time (t=0), when the first edge of pulse arrives at the surface, to the time ($t=\tau$) when the end edge of a pulse with a width of τ arrives at the surface, the received power increases linearly as shown in Figure 4.10.2. The received pulses are composed of echoes from various parts of the sea surface. Therefore the travel time from a satellite to the sea surface can be calculated by averaging the received pulses. Pulse compression techniques will be also applied (see 4.2) in order to obtain a high frequency pulse for improvement of the resolution.

Ocean wave height can be estimated if the relation between the average scattering coefficient and elapsed time as seen in the different gradients in Figure 4.10.3 is taken into account.

Table 4.10.1 compares the functions of four radar altimeters; Geosat-ALT/SALT (Spinsat Altimeter), ERS-1 RA (Radar Altimeter), TOPEX-ALT, and POSEIDON-ALT. Particularly one should note that TOPEX/POSEIDON-ALT's have very high accuracy of altimetry with ±2 cm and ±4cm respectively.

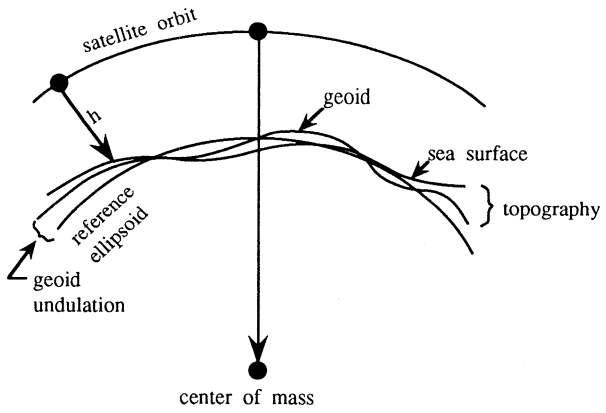

Fig.4.10.1 Principle of radar altimetry

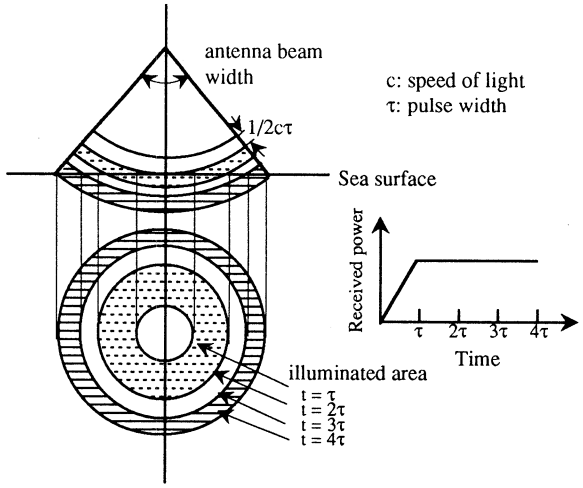

Fig.4.10.2 Change of illuminated area and received power

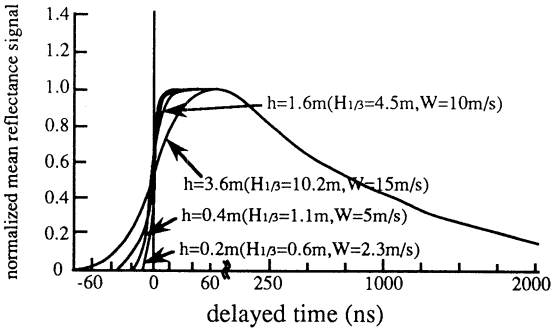

Figure 4.10.3 Averaged scattering coefficient of ocean wave [1)]

4.11 Measurement of Sea Wind

Measurement of the sea wind is not made directly but indirectly from two processes, that is, the microwave scattering from the sea surface and relationship between sea wind and wave height.There are two methods for measurement of sea wind.

a. to estimate the backscattering coefficient σ° using a microwave scatterometer
b. to measure the brightness temperature using a microwave radiometer

The following three models are used to estimate the backscattering coefficient σ° in the case of a microwave scatterometer.

a. **specular point model**
b. **Bragg model**
c. **composite surface model**

Figure 4.11.1 shows the relationship between backscattering cross section and the incident angle which has been obtained from the actual measurement. The specular point model can be applied to the region A in the figure, with the incident angle from 0° to 25°, where the sea clutter or sea roughness is much larger than the microwave wavelength. In this case, the backscattering coefficient σ° is proportional to the resultant probability density of x and y components of the gradient.

The Bragg model can be applied to the region B in the figure with the incident angle larger than 25°, where σ° decreases very gently except near 90°. This is called **Bragg scattering** which can be seen under the condition when the wavelengths of microwave and the sea wave have a similar spectrum. The ideal condition for Bragg scattering has the range from 25° to 65° with the wavelength of the capillary wave being from 1 cm to a few cm.

However, the actual sea surface is a composite of capillary waves and gravity waves for which the composite surface model has been developed but not yet verified theoretically. The second procedure is to estimate the sea surface condition from the backscattering coefficient . Figure 4.11.2 shows the correlation between variance of wave slope, S^2, and the wind velocity measured by Cox and Munk, which can be applied for the specular point model when σ° is given as a function of S^2. In the case of θ>25, it is found that the sea wind is proportional to the **spectral density**, but the models are still under development. Figure 4.11.3 shows the distribution of wind velocity and wind direction that was measured by SASS (Seasat-A Satellite Scatterometer) for the typhoon on Oct. 2, 1978. In the case of the microwave radiometer, the sea wind can be computed from the brightness temperature using the fact that the emissivity is a function of complex permittivity with parameters of salinity, sea clutter, sea temperature and bubbles. Two algorithms have been developed by Wentz and Wilheit for Seasat- SMMR for the sea wind velocity.

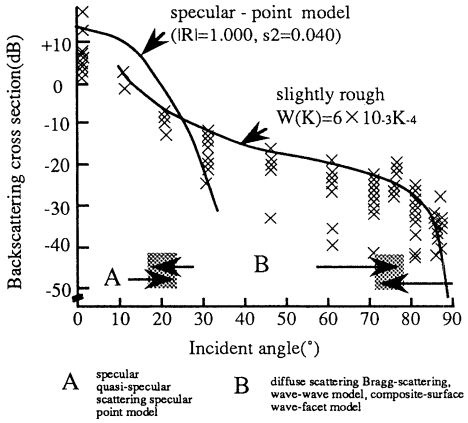

Figure 4.11.1 Relation between backscattering cross section and the incident angle (Valenzuela 1)

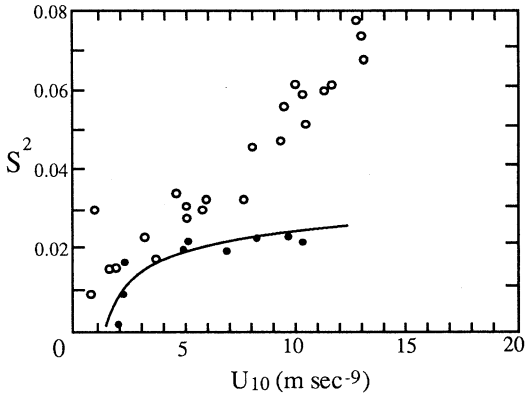

Figure 4.11.2 Correlations between variance of wave slope S and the wind velocity measured by Cox and Munk.

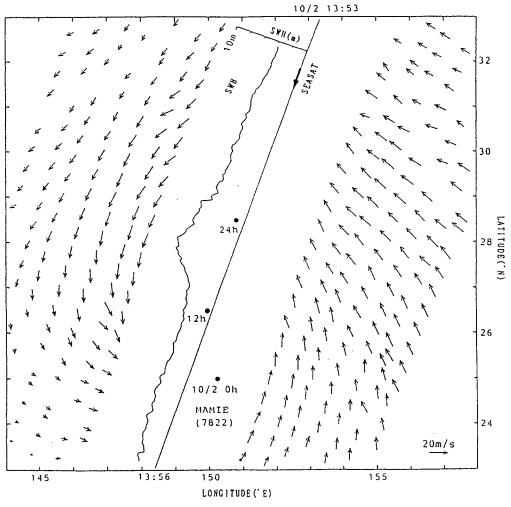

Figure 4.11.3 Distributions of the wind direction measured by SASS for the typhoon on OCT.2, 1978. 3)

(Black point in the Fig. shows the center of typhoon and SWH shows the sea surface change besides the typhoon monitored by Seasat-ALT.)

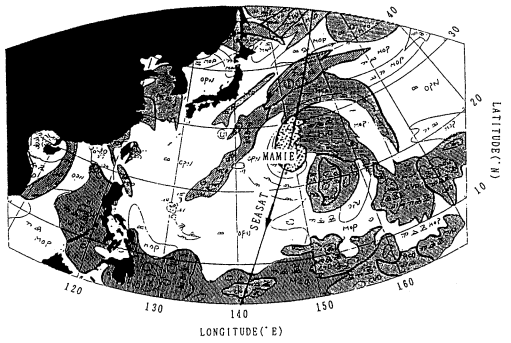

Figure 4.11.4 Cloud map on OCT.2,1973 analyzed by using GMS-1 data

4.12 Wave Measurement by Radar

While ordinary measurements of waves by a wave gauge are used for a time variation of wave height at a point, remote sensing techniques gives information over a broader area.

There are two methods of wave measurement used in remote sensing.
a. space borne sensors such as SAR and microwave altimeter
b. ground base radar such as **X band radar** and **HF Doppler radar**

As space borne sensors have a lower resolution (of the order of a few ten meters to a few kilometers), large size currents, typhoons over wide areas, global wave distribution, etc., will be better monitored by these systems.

On the other hand, ground based radar is suitable for monitoring the waves in near offshore or shallow zones, with the wave field of a few ten centimeters to a few hundred meters.

Figure 4.12.1 shows the distribution of average significant wave height which was measured by GEOSAT-ALT, with an accuracy of ±0.5 m or 10 % of the wave height.

Space borne SAR and ground based X band radar are used for measurement of reflectivity from the sea clutter at similar wavelengths to the sensors based on Bragg scattering (see 4.11).

Figure 4.12.2 explains the effect of **capillary waves** with respect to slope change or incident angle for Bragg scattering and wave height.

Figure 4.12.3 shows the sea surface conditions measured by SAR and X band radar. The measurement of wave direction and wave length is already operational as a ship borne radar but the measurement of wave height is still being researched. HF Doppler radar using high frequency band (10-100 m) , which is longer than microwave can measure the Bragg scattering from the sea clutter with wave lengths of 5-50 m.

Wave conditions such as wave direction, significant wave height, predominant wave, current etc. of **wind waves** with longer wave lengths, can be measured by using the Doppler effect with phase velocity of the wave crest. HF Doppler radar is already operational.

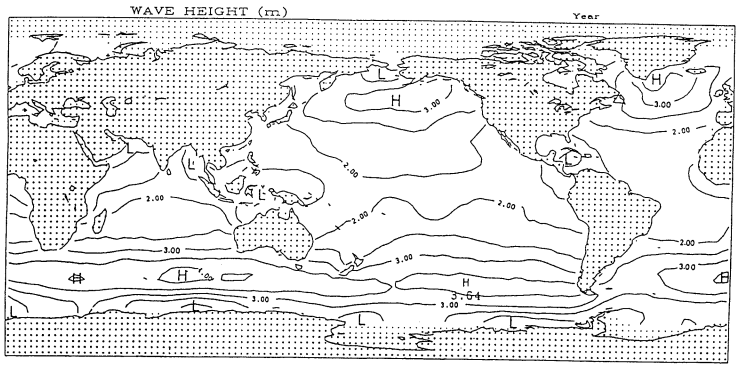

Figure 4.12.1 Distribution of average significant wave height measured by GEOSAT-ALT (courtesy of Japan Meteological Research Institute)

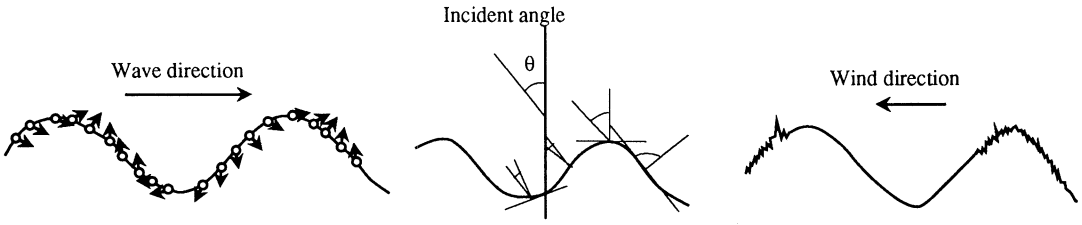

(a)Velocity bunching effect upon capillary wave by the wave particle motion
(b)Tilt modulation effect upon Bragg scattering condition
(c)Hydrodynamics modulation effect upon the wave development on each facet

Figure 4.12.2 Modulation effect of capillary waves.

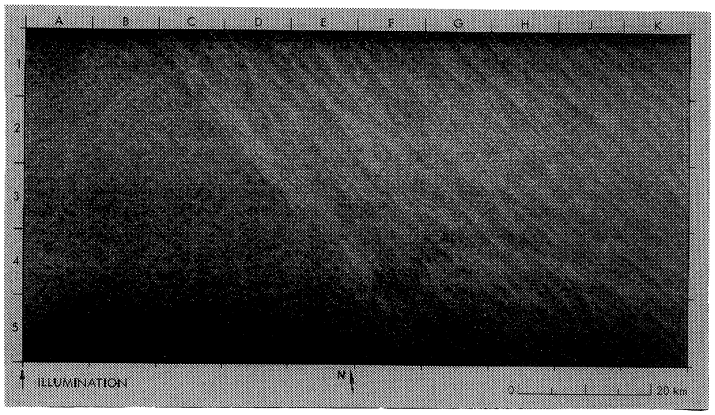

Figure 4.12.3 Sea surface condition measured by SIR-A (courtesy of NASA/JPL)

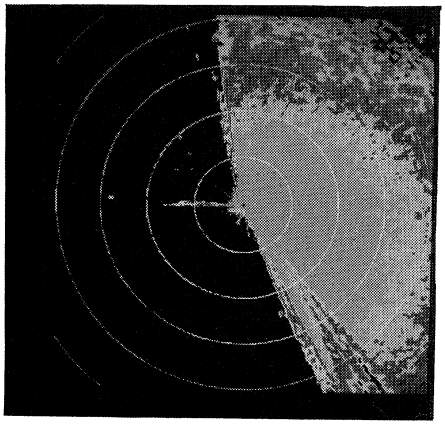

Figure 4.12.4 Sea surface condition measured by X-band radar (courtesy of Japan Meteological Research Institute)